

MODELING AND SIMULATION OF MODULATED TOOL PATH (MTP) TURNING STABILITY

Ryan W. Copenhaver^{1,2} and Tony L. Schmitz^{1,2}
¹Mechanical, Aerospace, and Biomedical Engineering
University of Tennessee, Knoxville
Knoxville, TN 37996, USA
²Energy and Transportation Science Division
Oak Ridge National Laboratory
Oak Ridge, TN 37830, USA

ABSTRACT

A time domain simulation for predicting stability during modulated tool path turning (MTP) is presented. Stability maps for MTP parameter pairs (oscillation magnitude and frequency) at selected chip widths are provided, where stability is determined using a periodic sampling-based metric. An AISI 1026 steel tube turning setup is used to complete MTP stability tests. It includes in-process measurements of cutting force, tool displacement, tool velocity, and a once-per-revolution signal. Predicted and measured signals are compared to verify simulation accuracy, including tests with and without MTP that demonstrate a change in stability for the same spindle speed and chip width.

INTRODUCTION

Conventional turning operations often exhibit uninterrupted cutting. This tends to produce a continuous chip that can wrap and collect near the cutting edge when machining ductile metals. The local buildup of this continuous chip can result in workpiece scratching, tool damage, machinist injury, and increased cycle time to clear the chips. Conventional chip management may use engineered rake face geometries [1] or high-pressure coolant directed at the rake face-chip interface [2], for example. Modulated tool path (MTP) turning offers an alternative approach, where discrete chips are formed by repeatedly interrupting the continuous chip formation using the machine axes to superimpose low frequency tool oscillations on the nominal tool feed motion. Prior MTP efforts have demonstrated broken chip length control. Stability behavior for MTP turning was also reported [3]. In this paper, a time domain simulation for MTP turning is described. This simulation is then used, together with a stability metric based on periodic sampling, to develop process stability maps. These stability maps are verified experimentally and compared to continuous turning (no MTP) performance.

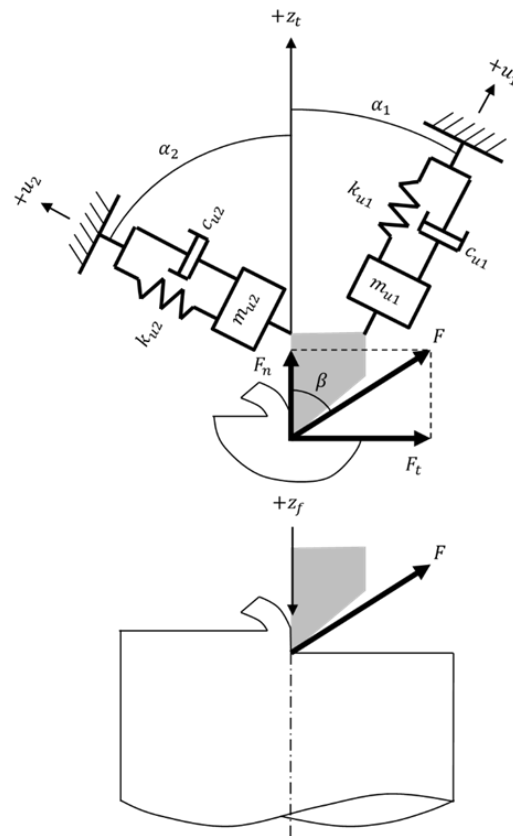


FIGURE 1. (Top) Flexible tool MTP turning dynamics model. The tangential, F_t , normal, F_n , and resultant force, F , components are identified, as well as the modal parameters that represent the structural dynamics in two orthogonal directions, u_1 and u_2 . The MTP feed motion, z_t , and tool vibration, z_t , are also identified. (Bottom) Model orientation for the tube turning tests completed in this study.

METHODOLOGY

In order to model the cutting force and tool vibration during MTP turning, a time domain simulation was developed. In each time step of the simulation, the instantaneous chip thickness is calculated by considering the current and previous surfaces. The

cutting force is then calculated using this chip thickness, the chip width, and cutting force model. Once the force is known, the second-order differential equations of motion for the flexible cutter are solved by numerical integration [4-5]. The corresponding tool displacement is then used together with the commanded MTP motion to calculate the chip thickness in the next time step.

For numerical integration using the semi-implicit Euler method, the requirement is that the time step is small enough to avoid numerical instability. For this study, the time step was selected to be 50 times smaller than the smallest vibration period for the structural dynamics. Given the time step, the simulation time vector and corresponding MTP feed motion, z_f , are described; see Fig. 1. The time vector, t , is defined from zero to the maximum simulation time in equal increments, dt . The MTP feed motion is then specified by Eq. 1:

$$z_f = \left(\frac{\Omega}{60} f_r\right) t + RAF \cdot f_r \cdot \sin\left(\frac{\Omega}{60} 2\pi \cdot OPR \cdot t\right), \quad (1)$$

where Ω is the spindle speed (rpm), f_r is the feed per revolution, RAF is the ratio of the MTP motion amplitude to the feed per revolution, and OPR is the number of sinusoidal MTP oscillations per revolution of the rotating part.

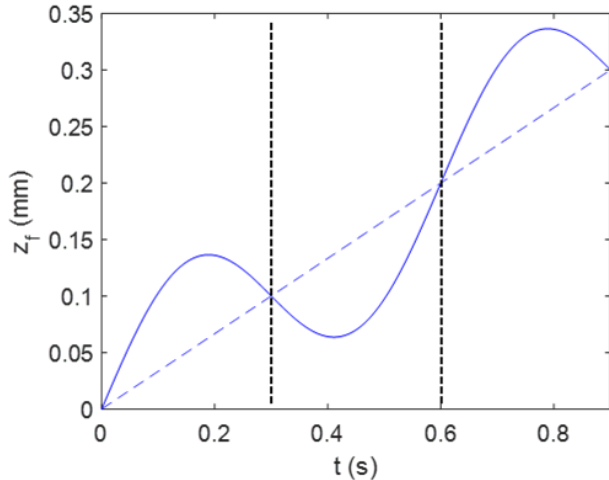


FIGURE 2. MTP feed motion for three spindle revolutions. The spindle speed is 200 rpm, the feed per revolution is 0.1 mm, and the RAF and OPR values are 0.8 and 0.5. The dashed, positive slope line identifies the constant feed, while the solid line shows its sum with the sinusoidal MTP contribution. The vertical dotted lines denote each revolution.

Figure 2 displays the MTP feed motion for a spindle speed of 200 rpm, a feed per revolution of 0.1 mm, and RAF and OPR values of 0.8 and 0.5, respectively.

In the figure, the dashed line denotes the constant feed advance of the tool into the part, while the solid line shows the superposition of the MTP oscillation onto the constant feed. The vertical dotted lines identify each revolution; three revolutions are plotted.

As noted, the first task in each simulation iteration is to calculate the instantaneous chip thickness. Fig. 3 aids in the calculation description by displaying the Fig. 2 data parsed by revolution. The revolution numbers are included on the right-hand side of the figure. The nominal chip thickness is the difference between the current tool position and the maximum value of all previous revolutions. Fig. 3 shows the chip thickness for revolution 2 as the hatched areas. The chip thickness is zero when the revolution 2 oscillation dips below the revolution 1 oscillation. The $+z_f$ direction is positive into the part, so “below” here means away from the part and no cutting occurs.

Figure 4 displays the chip thickness for revolution 3. Note that the instantaneous chip thickness is the difference between revolutions 3 and 1 for the time period between 0.0645 s and 0.2355 s and the difference between revolutions 3 and 2 for all other times. The corresponding chip thickness profile for the two revolutions is shown in Fig. 5. The two revolutions are segmented by the vertical dotted line. Because the OPR is 0.5 for this example, the chip thickness profile in Fig. 5 repeats every two revolutions in the absence of tool vibrations. MTP turning therefore exhibits periodic excitation, unlike traditional turning where the chip thickness and force are nominally constant.

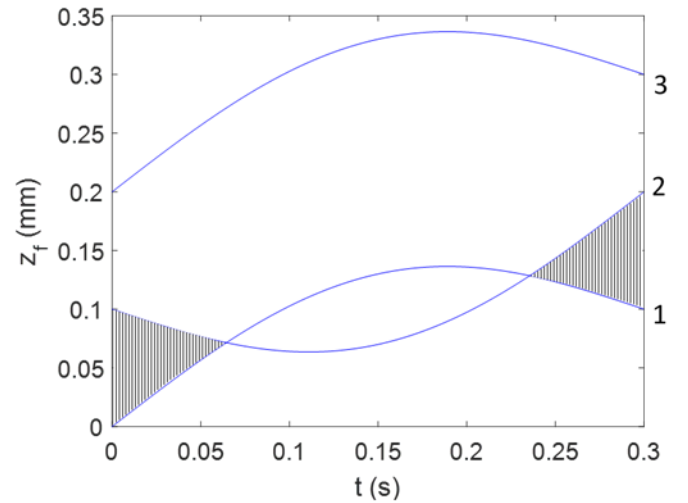


FIGURE 3. Chip thickness calculation for revolution 2. The nonzero chip thickness zones are denoted by the hatched areas.

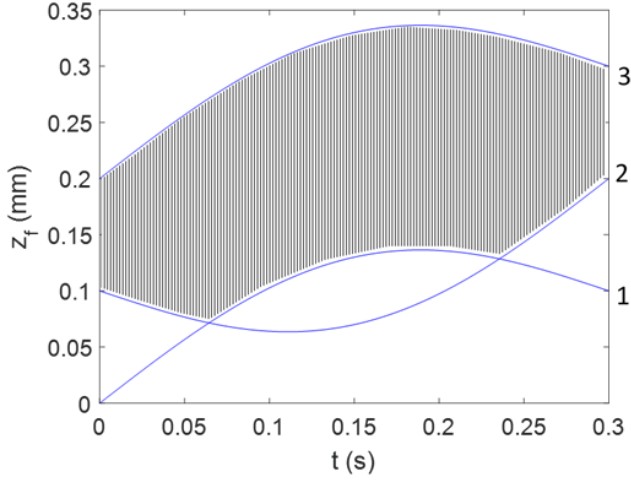


FIGURE 4. Chip thickness calculation for revolution 3. The instantaneous chip thickness is the difference between the current MTP motion and the maximum of all prior revolutions at the same rotation angle.

Figures 3 and 4 demonstrate the strategy for calculating the instantaneous chip thickness, h . Mathematically, this can be expressed as:

$$h = z_{f,n} - \max\{z_{f,n-1}, z_{f,n-2}, \dots\}, \quad (2)$$

where n is the current revolution. To include the tool dynamics, which are excited by the periodic forcing function displayed in Fig. 5, Eq. 2 must be augmented to include the effect of the tool displacement. If z_i is the tool displacement in the surface normal direction and it is considered positive out of the cut (see Fig. 1), then a positive tool displacement for the current revolution decreases the chip thickness. A positive tool displacement in a previous revolution, on the other hand, indicates that material that was intended to be removed was left behind. Therefore, a positive tool displacement for the maximum previous revolution yields a larger instantaneous chip thickness in the current revolution. Eq. 2 is updated to include the tool motion:

$$h = (z_{f,n} - z_{t,n}) - \max\{(z_{f,n-1} - z_{t,n-1}), (z_{f,n-2} - z_{t,n-2}), \dots\} \quad (3)$$

Returning to Fig. 5, the chip thickness is now calculated from Eq. 3 as shown in Eq. 4.

$$h = (z_{f,2} - z_{t,2}) - (z_{f,1} - z_{t,1}) = z_{f,2} - z_{f,1} - z_{t,2} + z_{t,1} \quad (4)$$

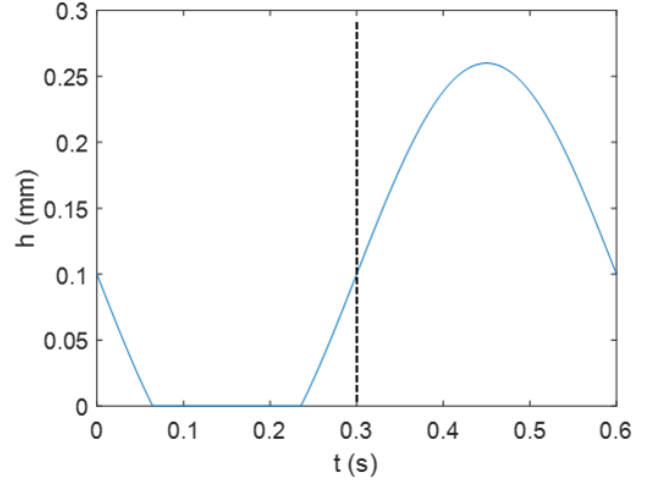


FIGURE 5. Instantaneous chip thickness for revolutions 2 and 3 considering the MTP motion only.

Equation 4 shows the effect of the tool vibrations directly. A positive $z_{t,2}$ reduces the current chip thickness, while a positive $z_{t,1}$ increases the current chip thickness. The final consideration is that Eqs. 2-4 can yield negative values, e.g., during the interval from 0.0645 s and 0.2355 s in Fig. 3. When $h < 0$, this indicates that no cutting occurs and the chip thickness is set equal to zero. This nonlinearly is incorporated in the numerical simulation.

Given the chip thickness, the cutting force is $F = K_s b h$, where K_s is the specific cutting force coefficient and b is the chip width. The resultant force is related to the tangential and normal direction force components through the force angle, β .

$$F_t = F \sin \beta = (K_s \sin \beta) b h = k_t b h \quad (5)$$

$$F_n = F \cos \beta = (K_s \cos \beta) b h = k_n b h \quad (6)$$

The resultant force is projected into the two mode directions to determine the corresponding displacements u_1 and u_2 .

$$F_{u1} = F \cos(\beta - \alpha_1) \quad (7) \quad F_{u2} = F \cos(\beta + \alpha_2) \quad (8)$$

$$\ddot{u}_1 = \frac{F_{u1} - c_{u1} \dot{u}_1 - k_{u1} u_1}{m_{u1}} \quad (9)$$

$$\dot{u}_1 = \dot{u}_1 + \ddot{u}_1 dt$$

$$u_1 = u_1 + \dot{u}_1 dt$$

$$\ddot{u}_2 = \frac{F_{u2} - c_{u2} \dot{u}_2 - k_{u2} u_2}{m_{u2}} \quad (10)$$

$$\dot{u}_2 = \dot{u}_2 + \ddot{u}_2 dt$$

$$u_2 = u_2 + \dot{u}_2 dt$$

The semi-implicit Euler integration procedure used to determine the current tool displacement components in the u_1 and u_2 directions proceeds according to Eqs. 9 and 10. In these two equations, m , c , and k are the modal mass, damping, and stiffness values, respectively, and the over-dots indicate time derivatives. Once u_1 and u_2 are known, they are projected into the surface normal direction to determine the new tool displacement.

$$z_t = u_1 \cos \alpha_1 + u_2 \cos \alpha_2 \quad (11)$$

To establish the MTP turning stability, periodic sampling was implemented [6], where the process signals are sampled at the forcing period. The discretized sampling period, SP , is defined in Eq. 12, where SR is the number of steps per revolution; see Eq. 13. If the process is stable, the sampled points repeat. If it is unstable, they do not repeat.

$$SP = \frac{SR}{OPR} \quad (12) \quad SR = \frac{60}{dt \cdot \Omega} \quad (13)$$

To automatically differentiate between stable (periodic) and unstable (secondary Hopf) conditions, the metric, M , was applied to the sampled points:

$$M = \frac{\sum_{i=2}^N |z_{ts}(i) - z_{ts}(i-1)|}{N} \quad (14)$$

where z_{ts} is the vector of once-per-MTP period sampled z_t displacements and N is the length of the z_{ts} vector [7]. For stable cuts, the M value is ideally zero (within the limits of numerical precision). For unstable cuts, however, $M > 0$. The use of this metric enables multiple simulations to be completed over a range of RAF and OPR values and a stability map to be automatically produced by plotting a single contour at an arbitrarily small M value.

RESULTS AND DISCUSSION

Turning experiments were completed on a Haas TL-1 CNC lathe. The tubular workpiece material was AISI 1026 steel. To keep a consistent surface speed, the workpieces were machined to have a mean diameter of 70 mm with varying wall thicknesses. Type C, 80° parallelogram carbide inserts with a zero rake angle, 7° relief angle, and a flat rake face were used. All experiments were conducted at a mean cutting speed of 122 m/min (556 rpm) with a nominal feed per revolution of 0.102 mm. Stability was controlled by varying the tube wall thickness (chip width) and RAF and OPR values.

Dynamic cutting forces were measured using a three-axis dynamometer (Kistler 9257B) mounted to the cross slide. A notch-type flexure was mounted to the

dynamometer. This flexure carried the carbide insert and acted as the cutting tool. A laser vibrometer (Polytec OFV-534/OFV-5000) was used to measure the feed direction, z_t , velocity of the cutting tool and a capacitance probe (Lion Precision C-18-13-2.0) was used to measure tool displacement, z_t . A laser tachometer was used to determine the actual spindle speed for periodic sampling at the MTP forcing frequency; see Fig. 6. The normal direction is aligned with the spindle axis, while the tangential direction is tangent to the cut surface (vertical). The tool's frequency response function was measured using impact testing. Modal fitting was completed to extract the modal mass, m , viscous damping, c , and stiffness, k , values for the simulation.

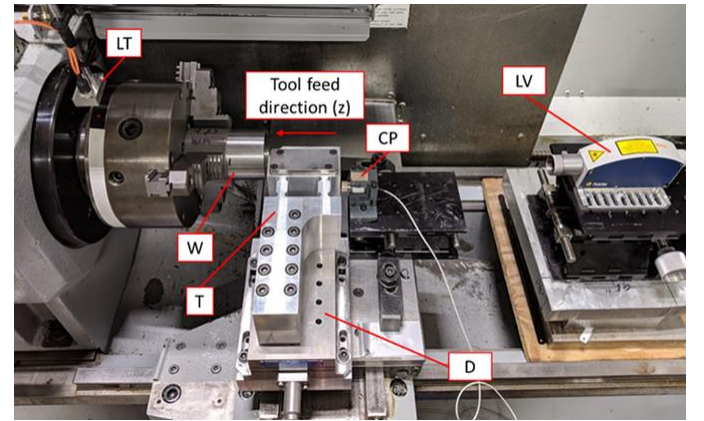


FIGURE 6. Photograph of tube turning setup including workpiece (W), dynamometer (D), flexure-based cutting tool (T), laser tachometer (LT), laser vibrometer (LV), and capacitance probe (CP).

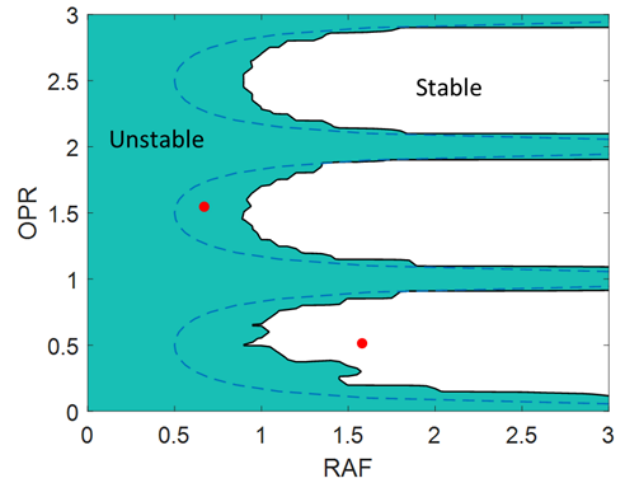


FIGURE 7. Stability map for $b = 4.5$ mm. Only selected $\{RAF, OPR\}$ pairs are stable for this chip width. Test points are denoted by dots.

The force model coefficients were identified from continuous (stable) cutting tests, where the force components in the normal and tangential directions were measured by the dynamometer for known chip thickness and width values. This process was repeated for decreasing chip thickness values until a continuous chip was no longer formed. The best fits to the measured forces are provided in Eqs. 14-15 (units are N/mm²).

$$k_n = -3355h^{0.81} + 2520 \quad (14)$$

$$k_t = -3490h^{0.22} + 4795 \quad (15)$$

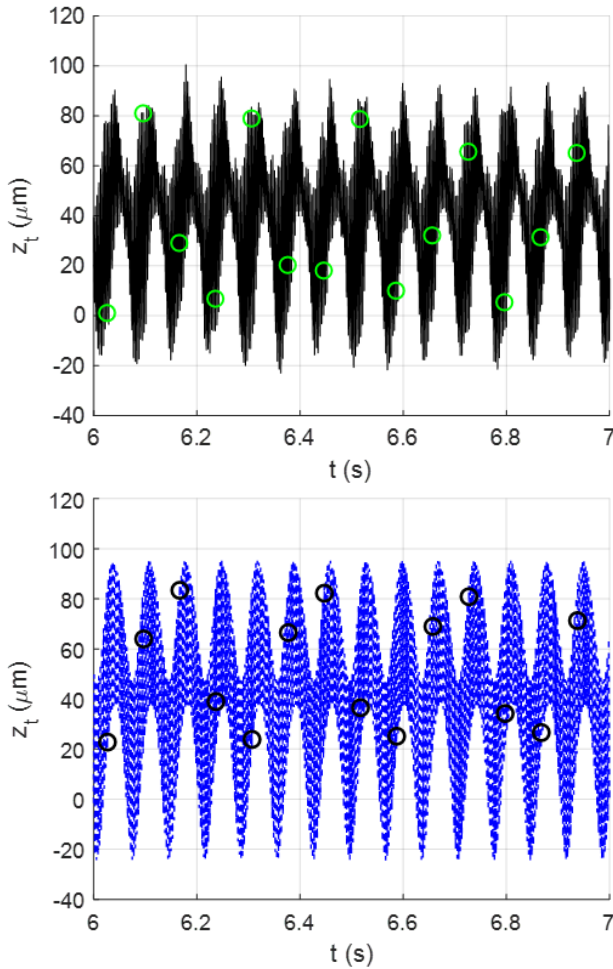


FIGURE 8. Measured (top) and predicted (bottom) tool displacement for $b = 4.5$ mm, $RAF = 0.65$, and $OPR = 1.54$. The result is unstable (chatter).

Time domain simulations were completed on a grid of $\{RAF, OPR\}$ pairs from 0 to 3 in steps of 0.05 for individual chip width values. The M value was computed for each pair and recorded. A stability map was then produced by plotting a single contour (solid

line) at $M = 1$ μm . Additionally, the analytical chip breaking limit [7] was superimposed on each stability map (dashed line); see Fig. 7. To verify the stability predictions, cutting tests were performed. Figure 8 displays the predicted and simulated tool motion with periodic samples (circles). The cut is unstable for the $\{0.65, 1.54\}$ pair, even though discontinuous chips were produced. With MTP parameters of $\{1.60, 0.50\}$, however, the cut is now stable; see Fig. 9. Cutting was unstable for no MTP conditions at $b = 4.5$ mm.

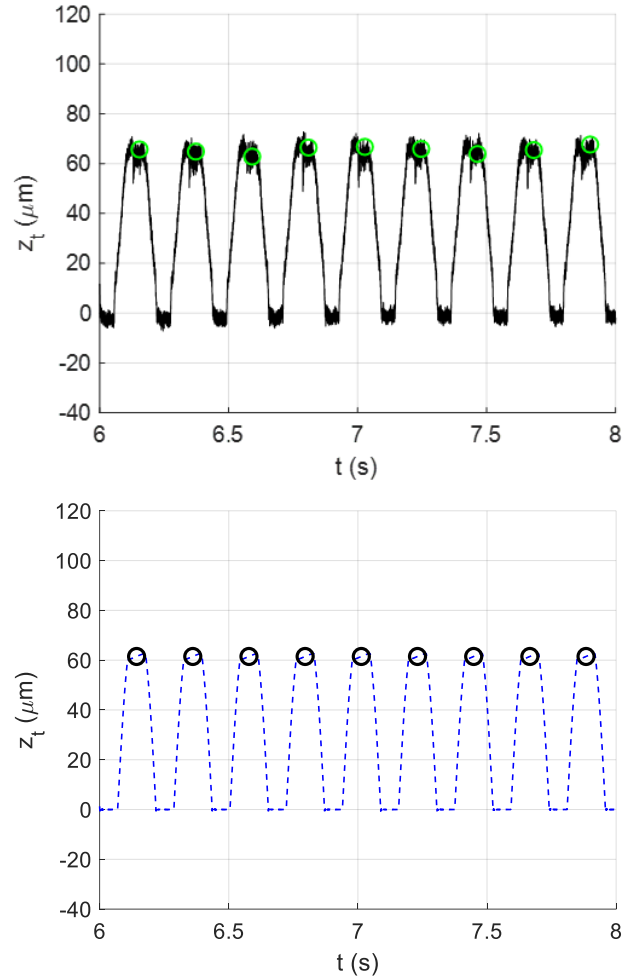


FIGURE 9. Measured (top) and predicted (bottom) tool displacement for $b = 4.5$ mm, $RAF = 1.60$, and $OPR = 0.50$. The result is stable.

CONCLUSIONS

A time domain simulation with periodic sampling for automated stability identification was implemented to produce stability maps for modulated tool path (MTP) turning. It was shown that either stable or unstable behavior can be obtained for the same spindle speed-chip width combination by varying only the MTP parameters. Predictions agreed with experiments.

ACKNOWLEDGEMENTS

This manuscript has been authored by UT-Battelle, LLC, under contract DE-AC05-00OR22725 with the US Department of Energy (DOE). The US government retains and the publisher, by accepting the article for publication, acknowledges that the US government retains a nonexclusive, paid-up, irrevocable, worldwide license to publish or reproduce the published form of this manuscript, or allow others to do so, for US government purposes. DOE will provide public access to these results of federally sponsored research in accordance with the DOE Public Access Plan (<http://energy.gov/downloads/doe-public-access-plan>).

REFERENCES

- [1] Jawahir IS. On the controllability of chip breaking cycles and modes of chip breaking in metal machining. *CIRP Annals* 1990;39/1: 47-51.
- [2] Rahman M, Kumar AS, Choudhury MR. Identification of effective zones for high pressure coolant in milling. *CIRP Annals* 2000;49/1: 47-52.
- [3] Copenhaver R, Smith S, Schmitz T. Stability analysis of modulated tool path turning. *CIRP Annals* 2018;67/1: 49-52.
- [4] Schmitz T, Smith S. *Mechanical Vibrations: Modeling and Measurement*. New York: Springer; 2012.
- [5] Schmitz T, Smith S. *Machining Dynamics: Frequency Response to Improved Productivity*. 2nd ed. New York: Springer; 2019.
- [6] Honeycutt A, Schmitz, T. A new metric for automated stability identification in time domain milling simulation. *Journal of Manufacturing Science and Engineering* 2016;138/7: 074501.
- [7] Mann JB, Guo Y, Saldana, C, Compton WD, Chandrasekar, S. Enhancing material removal processes using modulation-assisted machining. *Tribology International* 2011;44: 1225-1235.